Application Of The Z And Laplace Transforms To Panification Yeast Production Using An Airlift Bioreactor

Arnaldo Silva Oliveira (arnaldoufop@gmail.com)
Universidade Federal de São João del-Rei https://orcid.org/0000-0003-2588-7616
Juan C. B. Neto
Universidade Federal de Sao Joao del-Rei
Igor J. B. Santos
Universidade Federal de Sao Joao del-Rei
Edson R. Nucci
Universidade Federal de Sao Joao del-Rei

Research

Keywords: Saccharomyces cerevisiae, bioprocess, modeling, simulation

Posted Date: April 7th, 2020

DOI: https://doi.org/10.21203/rs.3.rs-20594/v1

APPLICATION OF THE Z AND LAPLACE TRANSFORMS TO PANIFICATION YEAST PRODUCTION USING AN AIRLIFT BIOREACTOR

Arnaldo S. Oliveira[1], Juan C. B. Neto[2], Igor J. B. Santos[3] and Edson R. Nucci[3]*

[1]Programa de Pós-Graduação em Engenharia Química (PPGEQ), [2]Chemical Engineering Department, [3]Chemistry, Biotechnology and Bioprocess Engineering Department, Universidade Federal de São João Del Rei, Brazil

Short running title: Z and Laplace transforms applied to a fermentation bioprocess

Corresponding author: Arnaldo S. Oliveira
PPGEQ/UFSJ
Campus Alto Paraopeba, Ouro Branco, MG
Zip code: 36420-000
Phone: 55 31 97505-0307
E-mail: arnaldoufop@gmail.com

Author: Edson R. Nucci
DQBIO/UFSJ
Campus Alto Paraopeba, Ouro Branco, MG
Zip code: 36420-000
E-mail: nucci@ufsj.edu.br

Author: Juan C. B. Neto
Chemical Engineering Department/UFSJ
Campus Alto Paraopeba, Ouro Branco, MG
Zip code: 36420-000
E-mail: coenqui@ufsj.edu.br

Author: Igor J. B. Neto
DQBIO/UFSJ
Campus Alto Paraopeba, Ouro Branco, MG
Zip code: 36420-000
E-mail: coenbio@ufsj.edu.br

List of abbreviations

$\dot{x} \rightarrow$	Variation of cell concentration over time
$\dot{S} \rightarrow$	Variation of substrate concentration over time
$dx/dt \rightarrow$	Variation of cell concentration over time
$dS/dt \rightarrow$	Variation of substrate concentration over time
$x(t) \rightarrow$	Cell concentration over time
$S(t) \rightarrow$	Substrate concentration in an instant t
$\mathcal{L} \rightarrow$	Laplace transform
$\alpha \rightarrow$	Dimensionless constant = $1/Y_{x/S}$
$\beta \rightarrow$	Dimensionless constant = $1/Y_{x/S}\, h$
$h \rightarrow$	Hour
$Z \rightarrow$	Z transform
$\mu \rightarrow$	Specific rate of cell growth
$\mu_{max} \rightarrow$	Maximum specific rate of cell growth
$\mu_{monod} \rightarrow$	Monod specific rate of cell growth
$\mu_{andrews} \rightarrow$	Andrews specific rate of cell growth
$K_S \rightarrow$	Saturation constant
$x \rightarrow$	Cell concentration
$x_{max} \rightarrow$	Maximum cell concentration
$x_0 \rightarrow$	Initial cell concentration
$x_n \rightarrow$	Cell concentration at time n
$x_{n+1} \rightarrow$	Cell concentration at time n+1
$x_i \rightarrow$	Cell concentration at time t_i
$S \rightarrow$	Substrate concentration
$S_0 \rightarrow$	Inicial substrate concentration
$S_n \rightarrow$	Substrate concentration at time n
$S_{n+1} \rightarrow$	Substrate concentration at time n+1

$K'_S \rightarrow$ Inhibition coefficient by the substrate

$V_{reactor} \rightarrow$ Reactor volume

$Y_{x/S} \rightarrow$ Conversion rate of substrate in cells

$t \rightarrow$ Time instant t

$t_i \rightarrow$ Initial time

$\dot{m}_{acumulated} \rightarrow$ Mass flow accumulated in the bioreactor

$\dot{m}_{in} \rightarrow$ Mass flow entering the bioreactor

$\dot{m}_{out} \rightarrow$ Mass flow out of the bioreactor

$\dot{m}_{generated} \rightarrow$ Mass flow generated by the process in the bioreactor

$\dot{m}_{consumed} \rightarrow$ Mass flow consumed by the process in the bioreactor

DECLARATIONS

Ethics approval and consent to participate – NOT APPLICABLE.

Consent for publication - NOT APPLICABLE.

Competing interests – THE AUTHORS DECLARE THAT THEY HAVE NO COMPETING INTERESTS.

Founding – NOT APPLICABLE

Authors contributions - ERN conceived of the study, and paticipated in its design and coordenation and helped to draft the manuscript. IJBS carried out the fermentation tests to obtain the data. JCBN developed the methodology for modeling the process. ASO adapted the equations and obtained the parameters by creating and simulating mathematical models and drafted the manuscript. All authors read and approved the final manuscript.

Acknowledgements – NOT APPLICABLE

Authors information

Arnaldo S. Oliveira

Master in Chemical Engineering from the Federal University of São João Del Rei and Bachelor in Metallurgical Engineering from the Federal University of Ouro Preto with eleven years of experience in project management at Reframax Eng. Ltda.

http://lattes.cnpq.br/4384133001094628

Edson R. Nucci

Graduated in Mathematics from the Federal University of São Carlos (2000), master's degree in Chemical Engineering from the Federal University of São Carlos (2003) and doctorate in Chemical Engineering from the Federal University of São Carlos (2007). He is currently professor I at the Federal University of São João Del-Rei. Has experience in the area of Chemical Engineering, with emphasis on Chemical Engineering and Bioprocesses, acting mainly on the following themes: Bioprocesses, Experimental planning, biotechnology, mathematical modeling and Intelligent Systems.

http://lattes.cnpq.br/4274582376583918

Igor J. B. Santos

Currently, professor in the Department of Chemistry, Biotechnology and Bioprocess Engineering at UFSJ-CAP. With a bachelor's degree and a degree in Chemistry from the Federal University of Viçosa with a technological emphasis, where he made the direct transition to the Doctorate in the area of Physical-Chemical concentration. Junior post-doctorate at the Operations and Processes Laboratory (LOP) of the Department of Food Technologies at the Federal University of Viçosa, with a CNPq scholarship. Develops research in the area of Nanotechnology and Thermodynamics, acting mainly on the following themes: nanostructures in packaging for preserving post-harvest fruits, nanostructures of whey proteins and protein conjugates to obtain new products, thermodynamics of nanotube interaction carbon, clays and oxides; polymer-surfactant interaction; two-phase aqueous system. He is currently a founding partner of Start up NanoPack - Technologies in packaging.

http://lattes.cnpq.br/9821155579435444

Juan C. B. Neto

Chemistry Technician from the Federal Technological Education Center of Minas Gerais (CEFET-MG), a degree in Chemical Engineering from the Federal University of Minas Gerais (1990), a master's degree in Metallurgical and Mining Engineering from the Federal University of Minas Gerais (1994) and PhD in Mechanical Engineering in the area of heat and fluids from UFMG (2012), acting mainly on the following topics: thermal and fluids, thermal machines, thermodynamics, modeling of dynamic systems, modeling of internal combustion engines and emissions, equipment assembly, animation computational process and equipment, computer simulation, unit operations.

http://lattes.cnpq.br/0529973259046894

APPLICATION OF THE Z AND LAPLACE TRANSFORMS TO PANIFICATION YEAST PRODUCTION USING AN AIRLIFT BIOREACTOR

Arnaldo S. Oliveira[1], Juan C. B. Neto[2], Igor J. B. Santos[3] and Edson R. Nucci[3]*

[1]Programa de Pós-Graduação em Engenharia Química (PPGEQ), [2]Chemical Engineering Department, [3]Chemistry, Biotechnology and Bioprocess Engineering Department, Universidade Federal de São João Del Rei, Brazil

Abstract. *The Z- and Laplace transforms are mathematical techniques applied to solve difference equations and differential equations, respectively. Mathematical models used to describe cell growth, substrate consumption and product formation in bioprocesses can be represented by these types of equations. Thus, in this work, the fermentation process of the yeast Saccharomyces cerevisiae was modeled using different models from the literature, and the Z- and Laplace transforms were applied to solve the equations. Once the equations were solved, the models were represented in state space and simulated in Octave® software. Finally, the models were compared to experimental data from previous studies and to each other. Verhulst was the model that best described the process, with an average error of 4.74% for cell growth and 13.9% for substrate consumption. This work is unprecedented since no works that use the Z transform and discrete models for the representation of fermentation of this yeast were found in the literature. Even more importantly, this work proved that discrete-time models can be applied to bioprocesses with the same precision as continuous-time models.*

Keywords: *Saccharomyces cerevisiae, bioprocess, modeling, simulation.*

Introduction

According to a report by Mcwillians [1] in BCC Research, the market for the yeast *Saccharomyces cerevisiae* will grow by 7.1% per year, from the current revenues of 7.6 billion dollars in 2017 to 10.7 billion dollars in 2022. Part of this increase in sales comes from the beverage market (beers, wines, etc.), which tends to show an average growth of 8.3% per year (driven by Asia and Latin America). The yeast market for bread (yeast) will grow 5.7% per year over the same period, from 4.4 to 5.8 billion dollars. Bioethanol, after being stagnant for a while, has a growth outlook of $124 million to $264 million, corresponding to 16.3 percent growth per year.

This scenario stimulates the development of studies aimed at optimizing processes. Many tools in the literature can be used to improve the productivity of a process, including mathematical modeling.

According to Finlayson [2], this technique is able to determine, based on experimental results, the best operating conditions for a process and, consequently, to predict the best operating conditions when some process parameters change. Many types of models can be applied to describe a process: linear models, nonlinear models, network models, multiobjective optimization and discrete models. After a model is established, it is necessary to simulate it. However, the mathematical resolution of these models is not always trivial, and in most cases, the use of mathematical techniques is necessary.

The Laplace transform method is very useful for solving ordinary differential equations. The Laplace transform allows the conversion of more complex functions into algebraic equations of a complex variable, "s", including the conversion of differential equations into algebraic equations. Once differential equations are transformed into algebraic equations, the necessary operations are performed on the domain "s" and then returned to the time domain by the inverse Laplace transform [3].

The Z-transform is widely used for discrete-time system analysis. It can be applied in linear differece equations, which, when converted to the Z domain, are transformed into algebraic equations that are easier to solve. After solving the algebraic equation in the Z domain, the inverse Z-transform is applied, thus providing the final system response [4]. It can be said that the Z-transform has the same function as the Laplace transform, except for discrete-time systems.

Although many studies have already been performed in the area of bioprocessing modeling, no work that has applied the Z-transform to construct discrete models for fermentation under the conditions studied in this work has been found in the literature. In this work, we applied different kinetic models found in the literature, in addition to the Z- and Laplace transforms, to the fermentation process of the yeast *Saccharomyces cerevisiae* and compared the results with experimental results and with each other.

Methodology

Yeasts play the major role in various processes in the food industry and in bioethanol production. The most commonly used yeast is *Saccharomyces cerevisiae*. In addition, other yeasts known as nonconventional yeasts (*Scheffersomyces stipitis*, *Yarrowia lipolytica*, *Kluyveromyces lactis* and *Dekkera bruxellensis*) are already being used in some processes [5]. Currently, there are many studies looking for alternative yeasts for the baking process; however, *Saccharomyces cerevisiae* still dominates the market.

Yeasts can metabolize glucose in two different ways: by oxidation or by fermentation. The oxidation mechanism provides cell growth, while fermentation provides the formation of ethanol. The metabolism of yeasts is influenced by oxygen and glucose concentrations; for example, a high concentration of glucose combined with a low concentration of oxygen may result in the Crabtree effect, which inhibits cell growth and favors the formation of ethanol [6]. *Saccharomyces cerevisiae* yeast shows cellular growth at both high and low oxygen concentrations, which is why it is so widely used [7].

Carbon and nitrogen are important sources of energy for *Saccharomyces cerevisiae* cells, and the availability and concentration of nitrogen can be associated with biosynthesis and ethanol; there are studies relating these effects [8].

Variations in temperature and pH impact the ethanol production in the fermentation process of *Saccharomyces cerevisiae* yeast [9]. A decrease in pH indicates a reduction in the formation of the product, whereas the inverse effect occurs with the temperature: the higher the temperature is, the smaller the amount of product formed.

Yeasts present six main phases of growth: lag phase, acceleration phase, log phase, deceleration phase, stationary phase and decline phase [10] [11] [12].

With regard to the operation regime, the fermentation process can be batch, semicontinuous or continuous [13]. According to Cinar [14], the batch process continues

to be the one most commonly applied in bioprocesses because it is less susceptible to contamination. The batch process consists of placing the inoculum and the culture medium in the bioreactor at the beginning of the process and removing the products only after the fermentation is completed; subsequently, the bioreactor is sterilized, and a new cycle begins.

Bioreactors can be divided into two main types: conventional bioreactors (stirred tank type and aerated mechanical agitation) and pneumatic bioreactors. Each bioreactor is better adapted to the culture of a certain species of microorganism [15]. Among the different types of pneumatic bioreactors is the concentric cylinder airlift type. In this type of bioreactor, the air is injected by the base through the central cylinder (riser) and is returned the base by the external cylinder (downcomer). The air promotes both the agitation of the culture medium and the aeration, with the advantage of causing less trauma to the cells and lower energy consumption than mechanical agitation bioreactors.

A model is nothing more than a dynamic relation between variables. There are many ways to represent the same mathematical model, but a given representation may apply better to one system than to another [16]. According to Aguirre [17], the most commonly used types of representation of mathematical models are transfer functions and state–space representations. As mentioned by Jacob and Zwart [18], representation in state space is able to describe the relationship among several variables (inputs and outputs), and its difference from the transfer function is its ability to establish general control strategies.

The simulation of continuous mathematical models involves the resolution of differential equations, while the simulation of discrete models involves the resolution of difference equations. To solve analytically linear differential equations, the Laplace transform is used, and to solve linear difference equations, the Z-transform is used [17].

Materials and methods

Modeling of the *Saccharomyces cerevisiae* fermentation process

Experimental data: The results from Ferreira *et al.* [19], who carried out four experiments in an airlift bioreactor, were used to calculate the parameters and compare the results of the models developed in this paper. The experiments were performed in a 6 L bioreactor at 32 ºC. Table 1 shows the experimental conditions of each experiment.

Table 1 Experimental conditions of the airlift bioreactor [19].

The curves for cell growth and substrate consumption of experiment 4, used to calculate the parameters and adjust all the models, are shown in Figure 2.

Fig 2. Experimental data obtained from a *Saccharomyces cerevisiae* culture on an airlift bioreactor with an initial substrate concentration of 10 $g.L^{-1}$, a gas and reactor volume proportion of 3 vvm, and an air flux of 15 $L.min^{-1}$ [8].

Microorganism: A fresh commercial yeast was utilized in this work. This yeast is found in baker's yeast or supermarkets that sells baker yeast. This kind of yeast (*Saccharomyces cerevisiae*) has 30% dry mass and 70% humidity [19].

Culture Media: The culture media were prepared in an appropriated recipient with distilled water, and the pH was regulated to 4.6 using acid. This media was sterilized in an autoclave with all necessary equipment and tools [8]. Table 2 shows the composition of the culture media.

Table 2 Composition of the culture media [19].

Process modeling: The process was modeled by three kinetic models, namely, those of Monod, Andrews and Verhulst. These models were solved in continuous and discrete time by using the Laplace and Z transforms, except for the Verhulst model. The ode 45 technique was applied on GNU Octave software, copyright © 1998 – 2018 John W. Eaton, to solve the continuous Verhulst model. Finally, to solve the Verhulst model in discrete time, the model equations were linearized, and the Z transform was applied to obtain the discrete model equations.

Model representation: The space state representation was used to solve the equation in the GNU Octave software.

Results and discussion

The first step was to apply the mass balance on the *Saccharomyces cerevisiae* fermentation process using the Monod kinetic model. After obtaining the Monod model equations, they were represented in a state space matrix as shown in Equation 5, which is the process representation for the continuous Monod kinetic model.

$$\begin{bmatrix}\dot{x}\\ \dot{S}\end{bmatrix} = \begin{bmatrix}\left(\frac{\mu_{max}S}{K_S+S}\right) & 0\\ -\left(\alpha\left(\frac{\mu_{max}S}{K_S+S}\right)+\beta\right) & 0\end{bmatrix}\begin{bmatrix}x\\ S\end{bmatrix} + \begin{bmatrix}0 & 0\\ 0 & 0\end{bmatrix}\begin{bmatrix}x_0\\ S_0\end{bmatrix} \qquad (5)$$

Equation 6 represents the same state space as Equation 5, but in discrete time. This model was obtained through the application of the Z transform to the continuous Monod equations.

$$\begin{bmatrix}x_{n+1}\\ S_{n+1}\end{bmatrix} = \begin{bmatrix}\left(1+\left(\frac{\mu_{max}S}{K_S+S}\right)\right) & 0\\ -\left(\alpha\left(\frac{\mu_{max}S}{K_S+S}\right)+\beta\right) & 1\end{bmatrix}\begin{bmatrix}x_n\\ S_n\end{bmatrix} + \begin{bmatrix}0 & 0\\ 0 & 0\end{bmatrix}\begin{bmatrix}x_0\\ S_0\end{bmatrix} \qquad (6)$$

The same methodology applied in the Monod model was also applied to the Andrews model. The state space for continuous and discrete time are represented in Equations 7 and 8, respectively.

$$\begin{bmatrix}\dot{x}\\ \dot{S}\end{bmatrix} = \begin{bmatrix}\left(\frac{\mu_{max}S}{K_S + S + \frac{S^2}{K'_S}}\right) & 0\\ -\left(\alpha\left(\frac{\mu_{max}S}{K_S + S + \frac{S^2}{K'_S}}\right) + \beta\right) & 0\end{bmatrix}\begin{bmatrix}x\\ S\end{bmatrix} + \begin{bmatrix}0 & 0\\ 0 & 0\end{bmatrix}\begin{bmatrix}x_0\\ S_0\end{bmatrix} \quad (7)$$

$$\begin{bmatrix}x_{n+1}\\ S_{n+1}\end{bmatrix} = \begin{bmatrix}\left(1 + \left(\frac{\mu_{max}S}{K_S + S + \frac{S^2}{K'_S}}\right)\right) & 0\\ -\left(\alpha\left(\frac{\mu_{max}S}{K_S + S + \frac{S^2}{K'_S}}\right) + \beta\right) & 1\end{bmatrix}\begin{bmatrix}x_n\\ S_n\end{bmatrix} + \begin{bmatrix}0 & 0\\ 0 & 0\end{bmatrix}\begin{bmatrix}x_0\\ S_0\end{bmatrix} \quad (8)$$

To solve the continuous Verhulst model, the differential Equations (9 and 10) and the ode 45 technique were applied. This model was not presented in state space representation because it is nonlinear.

$$\frac{dx}{dt} = \mu x - \frac{\mu x^2}{x_{máx}} \quad (9)$$

$$\frac{\mathrm{dS}}{\mathrm{dt}} = -\alpha\mu\mathrm{x} + \alpha\mu\frac{\mathrm{x}^2}{\mathrm{x_{máx}}} - \beta\mathrm{x} \quad (10)$$

The Z transform cannot be applied to a nonlinear model. To write the Verhulst model in discrete time, the continuous model was first linearized. Then, the Z transform was applied to the difference equations, and the state space for the discrete Verhulst model was obtained (Equation 11).

$$\begin{bmatrix} x_{n+1} \\ S_{n+1} \end{bmatrix} = \begin{bmatrix} \left(1 + \mu - 2\mu \frac{x^*}{x_{máx}}\right) & 0 \\ \left(-\alpha\mu + 2\alpha\mu \frac{x^*}{x_{máx}} - \beta\right) & 1 \end{bmatrix} \begin{bmatrix} x_n \\ S_n \end{bmatrix} + \begin{bmatrix} 0 & 0 \\ 0 & 0 \end{bmatrix} \begin{bmatrix} x_a \\ S_a \end{bmatrix} \qquad (11)$$

After obtaining the mathematical representations for the Monod, Andrews and Verhulst models, the next step was to calculate the parameters. Table 3 shows the values obtained for the parameters.

Table 3 Parameter values calculated for the models.

The continuous Monod model was plotted using all the parameter values. A comparison of the model and experiment 4 points is shown in Figure 3. For cell growth, which includes 2 h of fermentation, the experimental points are closer to the model curve than are the points after 2 h. For substrate consumption, the points are close to the model curve until the substrate concentration of the model curve reaches 0 $g.L^{-1}$.

Fig 3. Comparison of the continuous Monod model and the experimental points (Experiment 4).

Compared with the points of experiment 4, the same trend is observed for the discrete Monod model (Figure 4). Conceptually, the discrete model is more suitable for describing fermentation processes. These processes can describe population variations because individuals (in this case, cells) are always integer numbers, not fractions (for example, a population cannot contain 1000.5 cells).

Fig 4. Comparison of the discrete Monod model and the experimental points (Experiment 4).

Analyzing the Andrews models (Figure 5), the models (discrete and continuous) show a slower cell growth rate for 2 h of fermentation. The substrate consumption also decreases more slowly than do the experimental points until it reaches 0 $g.L^{-1}$.

Fig 5. Comparison of the Andrews models (discrete and continuous) and the experimental points (Experiment 4).

Finally, we analyze the Verhulst model. In contrast to the Monod and Andrews models, the trends of the continuous and discrete time are not similar in the Verhulst models. This difference occurred because the continuous model was linearized prior to applying the Z transform and obtaining the discrete models. The Z transform can only be applied to linear systems[5]. In Figure 6, all the points of experiment 4 are closer to the curves of the continuous model than are all the other models. By contrast, the trends seen from the Monod model are observed in the discrete Verhulst model, in which the points of cell growth are closer to the model curve for 2 h of fermentation.

Fig 6. Comparison of the Verhulst models (discrete and continuous) and the experimental points (Experiment 4).

The next step was to compare all continuous models and all discrete models. Figure 7 shows that even without calculating the accuracy of each model, the Verhulst model showed the best adjustment to the points of experiment 4 among the continuous and discrete models.

Fig 7. Comparison of all the continuous and discrete models.

To confirm the information observed in Figure 7, the medium error for each model was calculated. The results are shown in Table 4.

Table 4 Error comparison for the continuous and discrete Monod, Andrews and Verhulst models.

After the models were compared, the discrete and continuous Verhulst models were simulated for another initial condition, namely, a cell concentration of 1.2 $g.L^{-1}$ and a substrate concentration of 5 $g.L^{-1}$. The results were compared with experiments 1, 2 and 3. The results are shown in Figure 8. The Verhulst model showed the best accuracy for describing the Costa [20] xanthan gum work.

Fig 8. Simulation of the continuous and discrete Verhulst models for an initial cell concentration of 1.2 $g.L^{-1}$ and an initial substrate concentration of 5.0 $g.L^{-1}$, and comparison with experiments 1, 2 and 3.

Finally, the precisions of the continuous and discrete Verhulst models were calculated, and the results are shown in Figure 9.

Fig 9. Dispersion chart for the accuracy of the Verhulst model. The initial cell concentration was 1.2 $g.L^{-1}$, and the initial substrate concentration was 5.0 $g.L^{-1}$.

Conclusions

Although discrete representations are not largely applied to bioprocesses, this work shows that the discrete representation has the same accuracy as the continuous models do. This finding indicates that the Z transform can be applied to fermentation processes. The parameters obtained for the Saccharomyces cerevisiae culture on a batch process in an Airlift bioreactor were $\mu_{máx} = 0.81\ h^{-1}$ and $Y_{x/S} = 0.35\ g_{cel}.g_{sac}^{-1}$.

The linear models (continuous or discrete) describe the cell growth for two hours of fermentation and the substrate consumption until it is completely depleted. The Andrews model does not accurately describe this process because it does not account for substrate inhibition.

The model that best represents this process is the nonlinear Verhulst model, as observed in a similar process by Costa [20], with a medium error of 0.166 $g.L^{-1}$ for cell growth and 0.346 $g.L^{-1}$ for substrate consumption. When the initial conditions were changed, the precision of the Verhulst model did change, but it still satisfactorily represented the process (Figure 9).

Acknowledgements

The authors thank UFSJ and the Fundação de Amparo à Pesquisa do Estado de Minas Gerais (FAPEMIG) for their financial support.

References

1. McWillians A, Yeasts, yeasts extracts, autolysates and related products: The global market. *BBC research report overview*, **9**: 1-9 (2017).
2. Finlayson BA, Introduction to chemical engineering computing, *Wiley interscience*, New Jersey: John Wiley and Sons **20**: 89-108 (2006).
3. Santos J, Laplace transforms: dynamic models, FCA, **14**: 6-19 (2005).
4. Artuzy Jr WA, Cruz RRW, Z transform introduction, UFPR, **16**: 1-16 (2010).
5. Steensels J, Snoek T, Meersman E, Nicolino MP, Voodeckers K, Verstrepen KJ, Improving industrial yeast strains: exploiting natural and artificial diversity, FEMS Microbiology Reviews, **49**: 947-995 (2014).
6. Ji M, Miao Y, Chen JU, You Y, Liu F, Xu L, Growth characteritics of freeze-tolerant baker's yeast Saccharomyces cerevisiae AFY in aerobic batch culture. Springerplus, **13**: 1-13 (2016).
7. Berry DR, Brown C, Physiology of yeast growth. In: Berry DR, Russel I, Stewart GG. Yeast Biotechnology. Springer (1987).
8. Marin IKO, Perez LAM, Garcia MC, Almendárez BEG, Hernández JCG, Gonzalez CR, Interactions between carbon and nitrogen sources depend on RIM15 and determine fermentative or respiratory growth in Saccharomyces cerevisiae. Springer-Verlag GmbH, **13**: 4535-4548 (2018).
9. Lu Y, Voon MKW, Huang D, Lee P, Liu S, Combined effects of fermentation temperature and pH on kinetic changes of chemical constituents of durian wine fermented with Saccharomyces cerevisiae. Appl Microbiol Biotechnol, **10**: 3005-3014 (2017).
10. Oliveira ARM, Aplicação de delineamentos fatoriais e metodologia de superficie de resposta para otimização de meio de cultura. UFSJ, **55**: 1-55 (2013).
11. Bredjing J, Jespersen L, Protein expression during lag phase and growth initiation in Saccharomyces cerevisiae. International Journal of Food Microbiology, **12**: 27-38 (2002).
12. Tuite MF, Oliver SG, Saccharomyces. Biotechnology Handbooks, Springer, Boston, 34: 249-282 (1991).
13. Kent JA, Industrial Fermentation: Principles, Process and Products. Handbook of Industrial Chermistry, Springer, Boston MA, **71**: 916-986 (1992).
14. Cinar A, Parulekar SJ, Undey C, Birol G, Batch Fermentation: Modeling, Monitoring and Control. Chicago: Marcel Dekker Inc., **2**: 4-5 (2003).
15. Gupta VK, New and Future Developments in Microbial Biotechnology and Bioengineering. Handbook of Industrial Chemistry: Aspergillus System Properties and Applications, Elsevier, **14**: 241-254 (2016).
16. Nidmeijer H, Schumacher JM, Three Decades of Mathematical System Theory. Lecture Notes in Control and Information Sciences, Springer, 97: 382-407 (1989).
17. Aguirre LA, Introduction to systems identification: linear and nonlinear techniques. 4th edition, Belo Horizonte, UFMG, **6**: 59-64 (2015).

18. Jacob B, Zward HJ, Linear Port-Hamiltonian Systems on Infinite-dimensional Spaces, Springer Basel, **2**: 14-15 (2002).

19. Ferreira AE, Nucci ER, Cruz AJG, Cerri MO, Comparing the performance of conventional and airlift bioreactor during the *Saccharomyces cerevisiae* cultivation. *Congress paper CHISA,* **1**: (2014).

20. Costa MRMF, Application of surface response methodology, kinetic models and Z transform on biopolymers production using alternative substrates. Master's degree work, UFSJ, **24**: 78-91 (2016).

LIST OF FIGURES

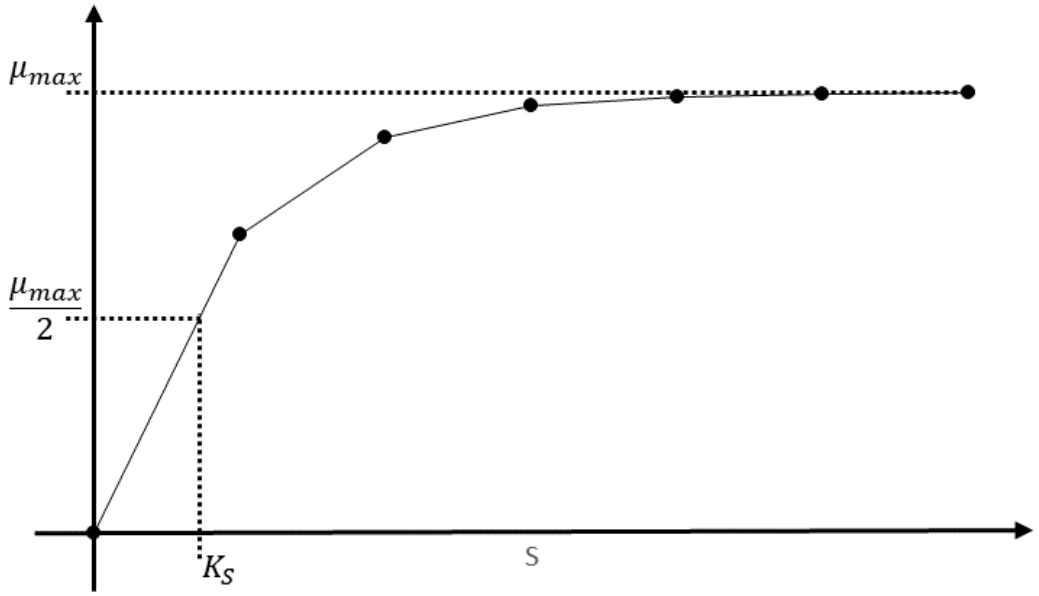

Fig 1. General curve for cell growth variation as a function of the substrate concentration from Braga[12].

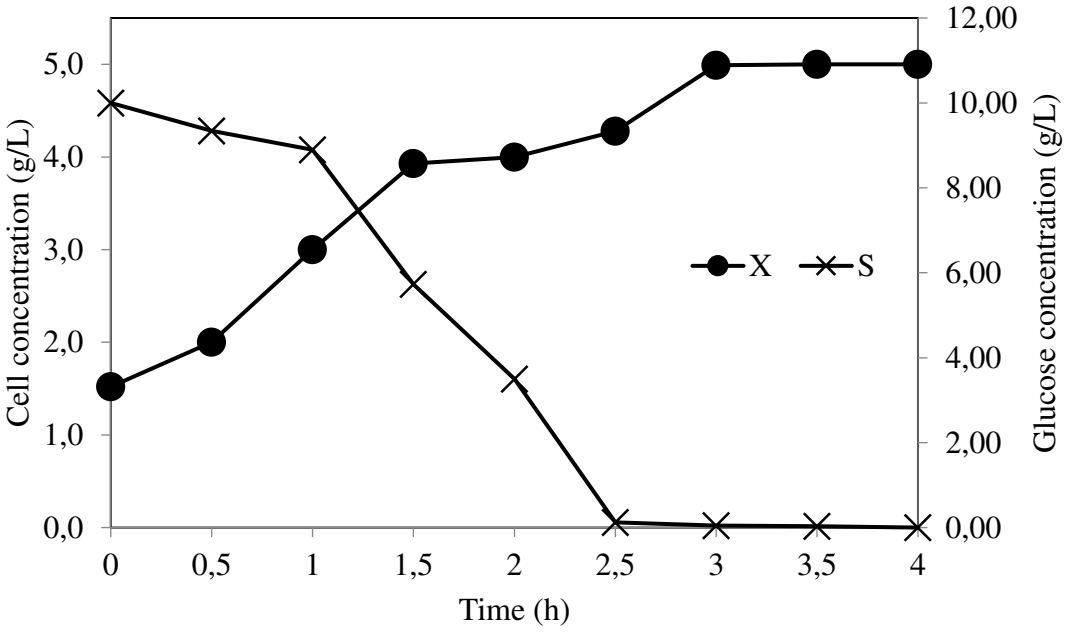

Fig 2. Experimental data obtained from a *Saccharomyces cerevisiae* culture on an airlift bioreactor with an initial substrate concentration of 10 $g.L^{-1}$, a gas and reactor volume proportion of 3 vvm, and an air flux of 15 $L.min^{-1}$ [8].

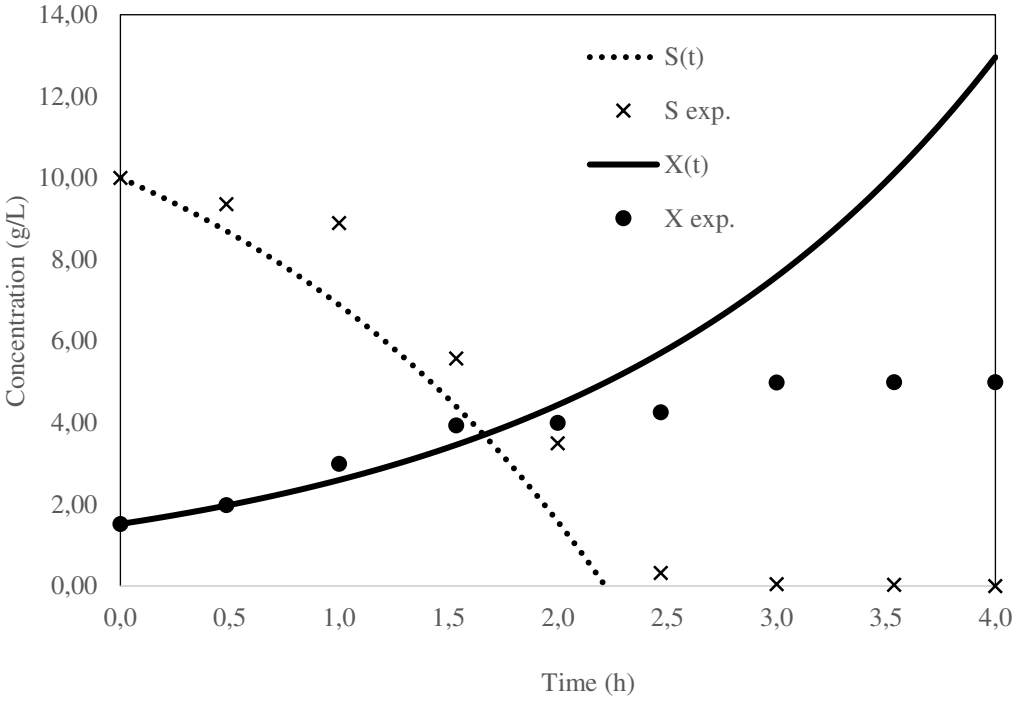

Fig 3. Comparison of the continuous Monod model and the experimental points (Experiment 4).

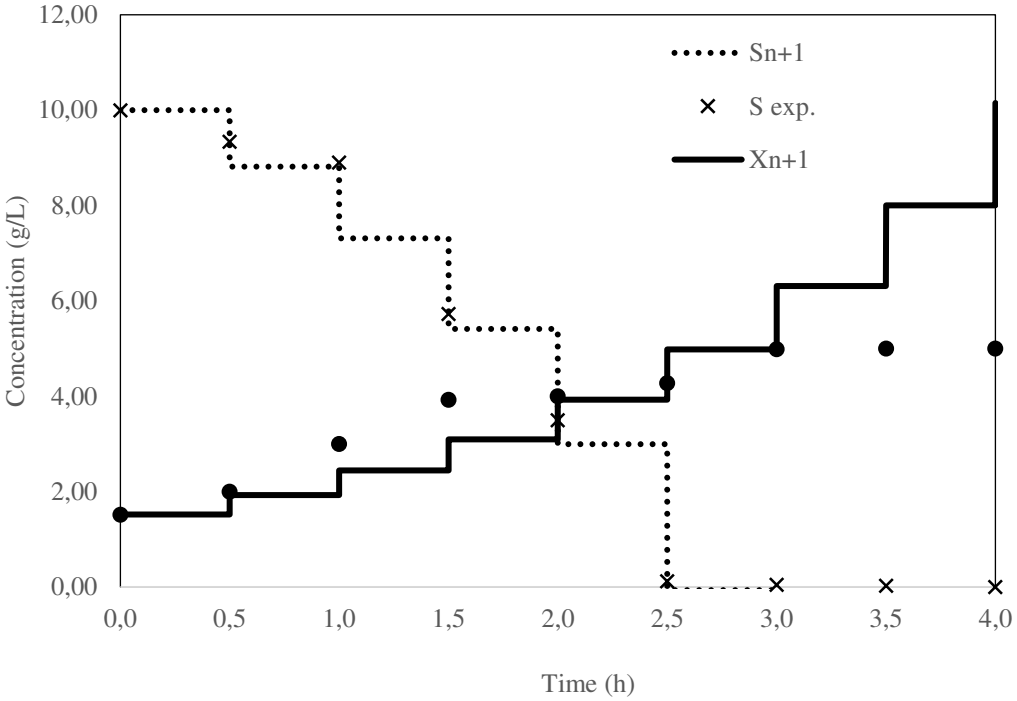

Fig 4. Comparison of the discrete Monod model and the experimental points (Experiment 4).

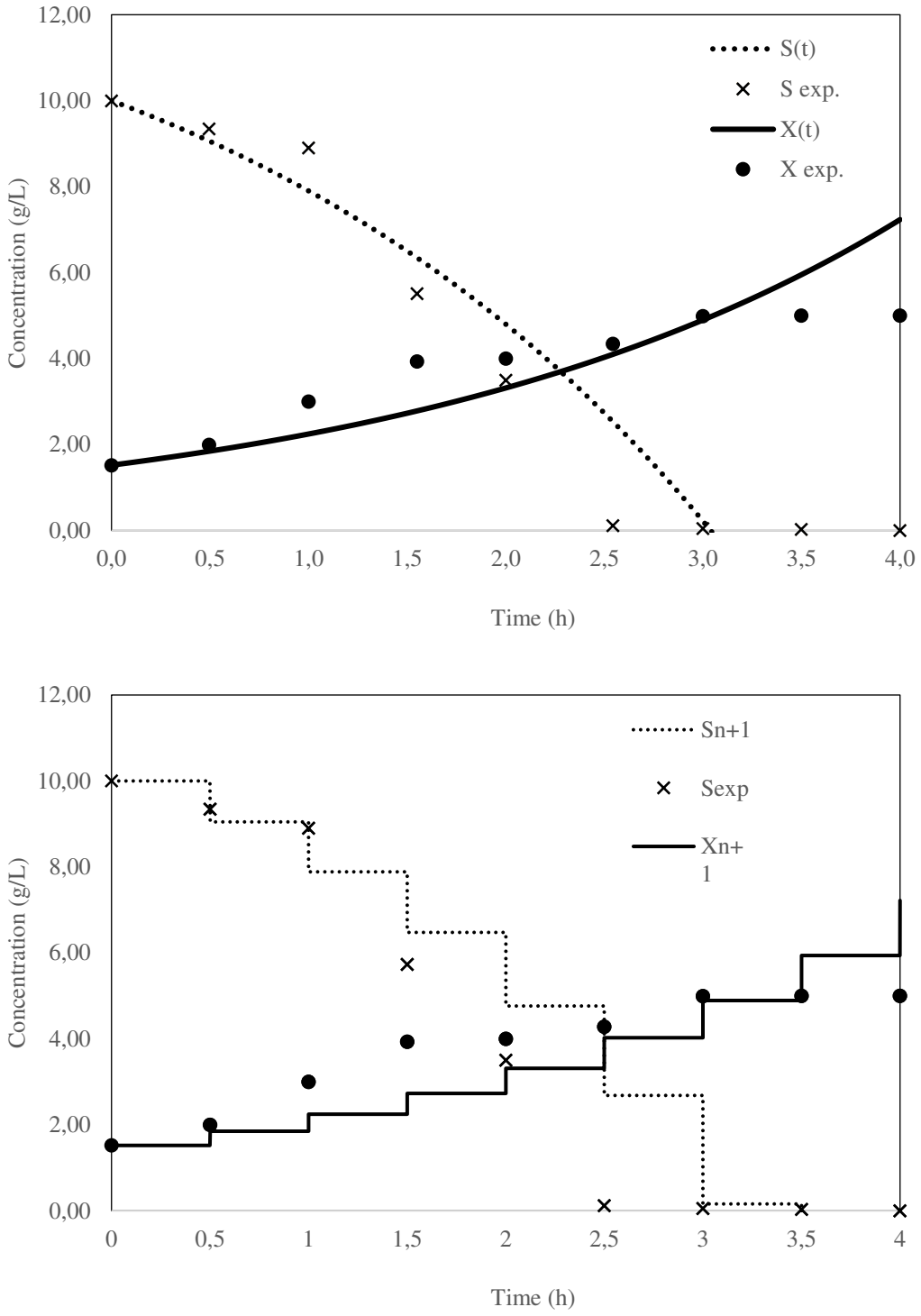

Fig 5. Comparison of the Andrews models (discrete and continuous) and the experimental points (Experiment 4).

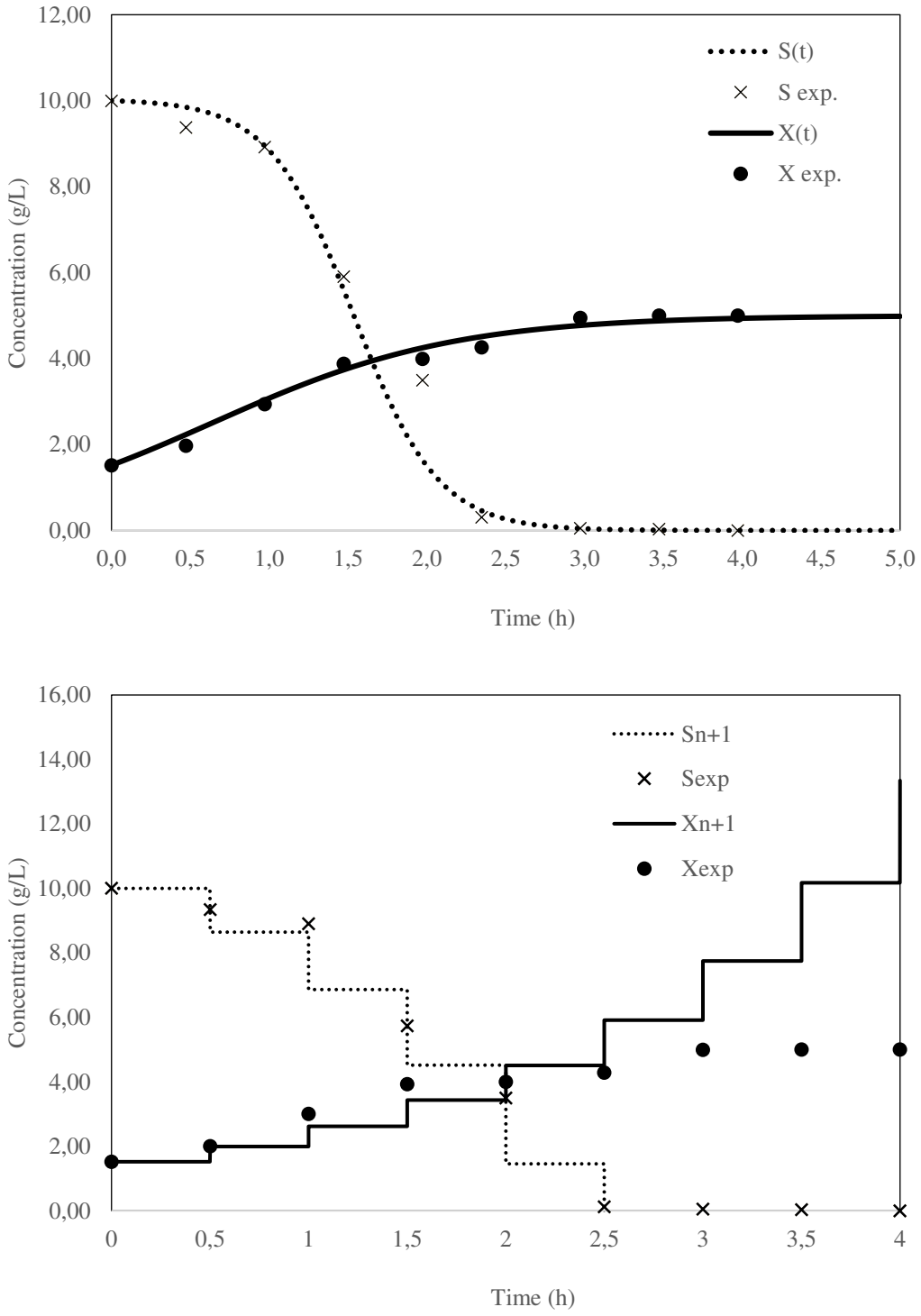

Fig 6. Comparison of the Verhulst models (discrete and continuous) and the experimental points (Experiment 4).

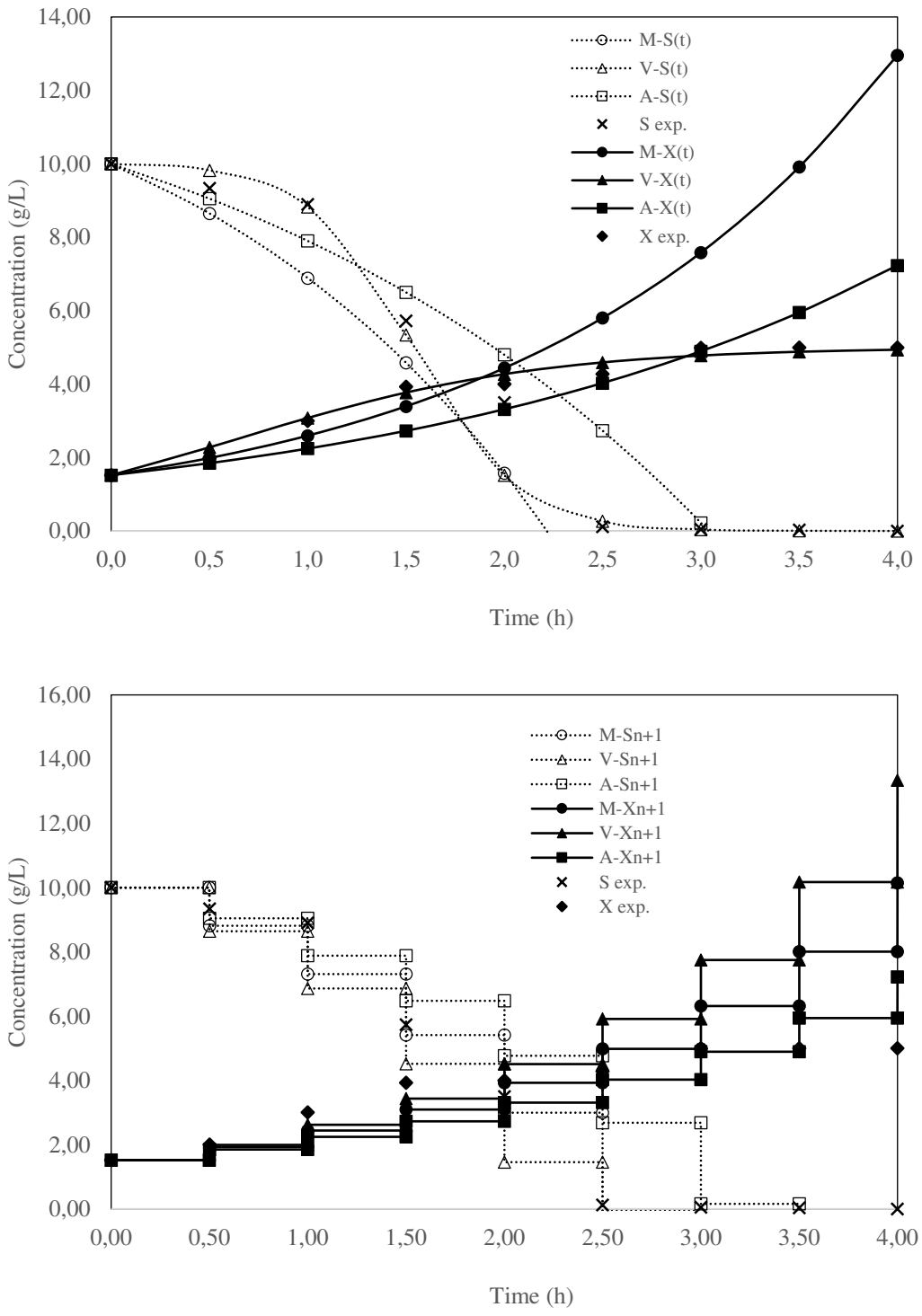

Fig 7. Comparison of all the continuous and discrete models.

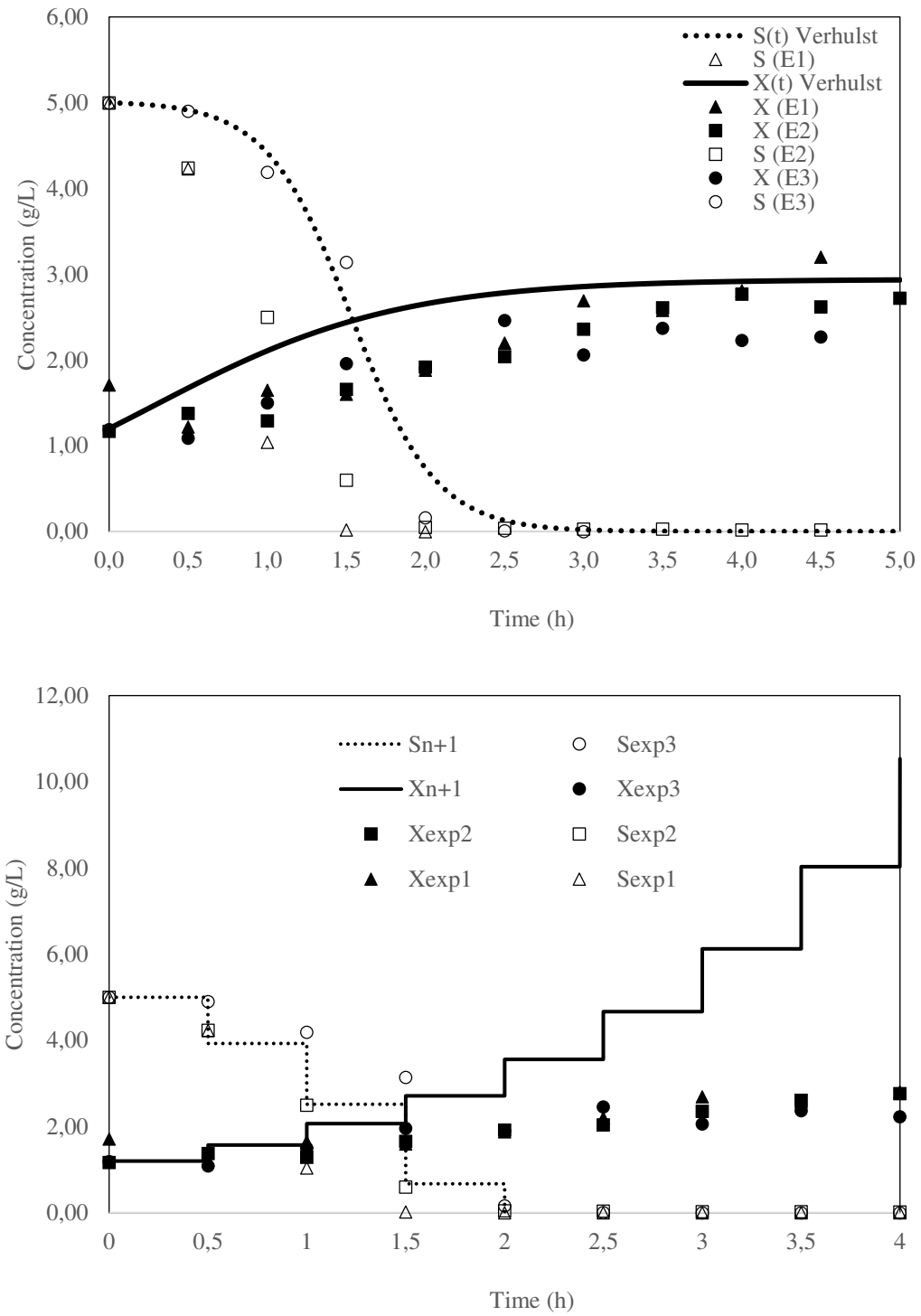

Fig 8. Simulation of the continuous and discrete Verhulst models for an initial cell concentration of 1.2 $g.L^{-1}$ and an initial substrate concentration of 5 $g.L^{-1}$ and comparison with experiments 1, 2 and 3.

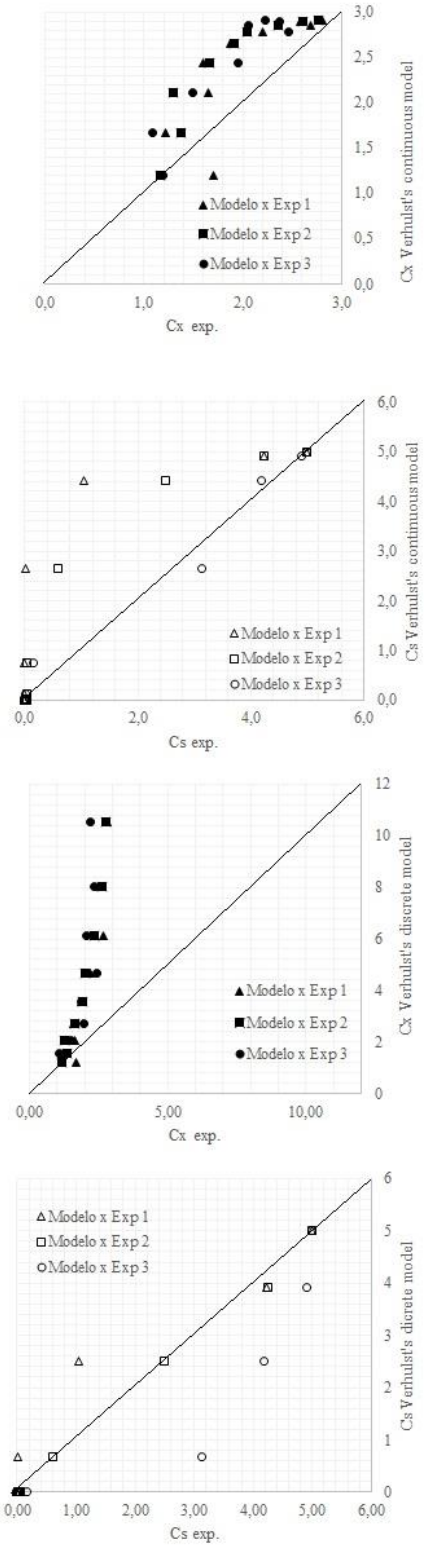

Fig 9. Dispersion chart for the accuracy of the Verhulst model. The initial cell concentration is 1.2 $g.L^{-1}$, and the initial substrate concentration is 5 $g.L^{-1}$.

FIGURE LEGENDS

Fig 1. General curve for cell growth variation as a function of the substrate concentration from Braga[12].

Fig 2. Experimental data obtained from a *Saccharomyces cerevisiae* culture on an airlift bioreactor with an initial substrate concentration of 10 $g.L^{-1}$, a gas and reactor volume proportion of 3 vvm, and an air flux of 15 $L.min^{-1}$ [8].

Fig 3. Comparison of the continuous Monod model and the experimental points (Experiment 4).

Fig 4. Comparison of the discrete Monod model and the experimental points (Experiment 4).

Fig 6. Comparison of the Verhulst models (discrete and continuous) and the experimental points (Experiment 4).

Fig 7. Comparison of all the continuous and discrete models.

Fig 8. Simulation of the continuous and discrete Verhulst models for an initial cell concentration of 1.2 $g.L^{-1}$ and an initial substrate concentration of 5 $g.L^{-1}$ and comparison with experiments 1, 2 and 3.

Fig 9. Dispersion chart for the accuracy of the Verhulst model. The initial cell concentration is 1.2 $g.L^{-1}$, and the initial substrate concentration is 5 $g.L^{-1}$.

LIST OF TABLES

Table 1 Experimental conditions of the airlift bioreactor.

	Airlift bioreactor	
Experiment	Air flow ($L.m^{-1}$)	Substrate concentration ($g.L^{-1}$)
1	15	5
2	10	5
3	5	5
4	15	10

Source: Adapted from Cerri *et al.*[8].

Table 2 Composition of the culture media.

pH	Glucose	KH_2PO_4	$MgSO_47H_2O$	Yeast extract	$(NH_4)_2SO_4$	Distilled water	Surfynol
4.6	10.0 $g.L^{-1}$	5.0 $g.L^{-1}$	0.5 $g.L^{-1}$	1.5 $g.L^{-1}$	4.0 $g.L^{-1}$	-	1.0 mL

Source: Adapted from Cerri *et al.*[8].

Table 3 Parameter values calculated for the models.

Parameter	Unit	Estimation
$\mu_{máx}$	($L.h^{-1}$)	0.8109* e 1.3**
K_S	($g.L^{-1}$)	5.1360
K'_S	($g.L^{-1}$)	42.1577
α	Dimensionless	2.8649
β	Dimensionless	0.0120
μ_{Monod}	(h^{-1})	0.5357
$\mu_{Andrews}$	(h^{-1})	0.48

*$\mu_{máx} = 0.8109$ was applied for the Andrews and Monod models.
**$\mu_{máx} = 1.3$ was applied for the Verhulst model.

Table 4 Error comparison for the continuous and discrete Monod, Andrews and Verhulst models.

Continuous cell growth models.

Time (h)	Experimental data	Monod		Verhulst		Andrews	
		Value	Error	Value	Error	Value	Error
0	1.520	1.520	0.000	1.520	0.000	1.520	0.000
0.5	2.000	1.987	-0.013	2.278	0.278	1.847	-0.153
1	3.000	2.597	-0.403	3.078	0.078	2.245	-0.755
1.5	3.930	3.396	-0.534	3.770	-0.160	2.729	-1.201
2	4.000	4.438	0.438	4.272	0.272	3.316	-0.684
2.5	4.280	5.803	1.523	4.592	0.312	4.030	-0.250
3	4.990	7.584	2.594	4.778	-0.212	4.897	-0.093
3.5	5.000	9.916	4.916	4.882	-0.118	5.950	0.950
4	5.000	12.959	7.959	4.938	-0.062	7.233	2.233

Continuous substrate consumption models.

Time (h)	Experimental data	Monod		Verhulst		Andrews	
		Value	Error	Value	Error	Value	Error
0	10.000	10.000	0.000	10.000	0.000	10.000	0.000
0.5	9.340	8.651	-0.689	9.823	0.483	9.052	-0.288
1	8.900	6.889	-2.011	8.826	-0.074	7.901	-0.999
1.5	5.730	4.584	-1.146	5.340	-0.390	6.500	0.770
2	3.500	1.574	-1.926	1.517	-1.983	4.800	1.300
2.5	0.120	-2.366	-2.486	0.269	0.149	2.731	2.611
3	0.050	-7.508	-7.558	0.043	-0.007	0.220	0.170
3.5	0.030	-14.241	-14.271	0.007	-0.023	-2.829	-2.859
4	0.000	-23.027	-23.027	0.001	0.001	-6.544	-6.544

Discrete cell growth models.

Time (h)	Experimental data	Monod		Verhulst		Andrews	
		Value	Error	Value	Error	Value	Error
0	1.520	1.520	0.000	1.520	0.000	1.520	0.000
0.5	2.000	1.927	-0.073	1.994	-0.006	1.847	-0.153
1	3.000	2.443	-0.557	2.616	-0.384	2.244	-0.756
1.5	3.930	3.098	-0.832	3.433	-0.497	2.726	-1.204
2	4.000	3.928	-0.072	4.504	0.504	3.312	-0.688
2.5	4.280	4.980	0.700	5.909	1.629	4.025	-0.255

Substrate consume discrete models.

Time (h)	Experimental data	Monod		Verhulst		Andrews	
		Value	Error	Value	Error	Value	Error
0	10.000	10.000	0.000	10.000	0.000	10.000	0.000
0.5	9.340	8.815	-0.525	8.641	-0.699	9.046	-0.294
1	8.900	7.313	-1.587	6.859	-2.041	7.886	-1.014
1.5	5.730	5.409	-0.321	4.520	-1.210	6.477	0.747
2	3.500	2.994	-0.506	1.452	-2.048	4.765	1.265
2.5	0.120	-0.067	-0.187	-2.574	-2.694	2.685	2.565

Figures

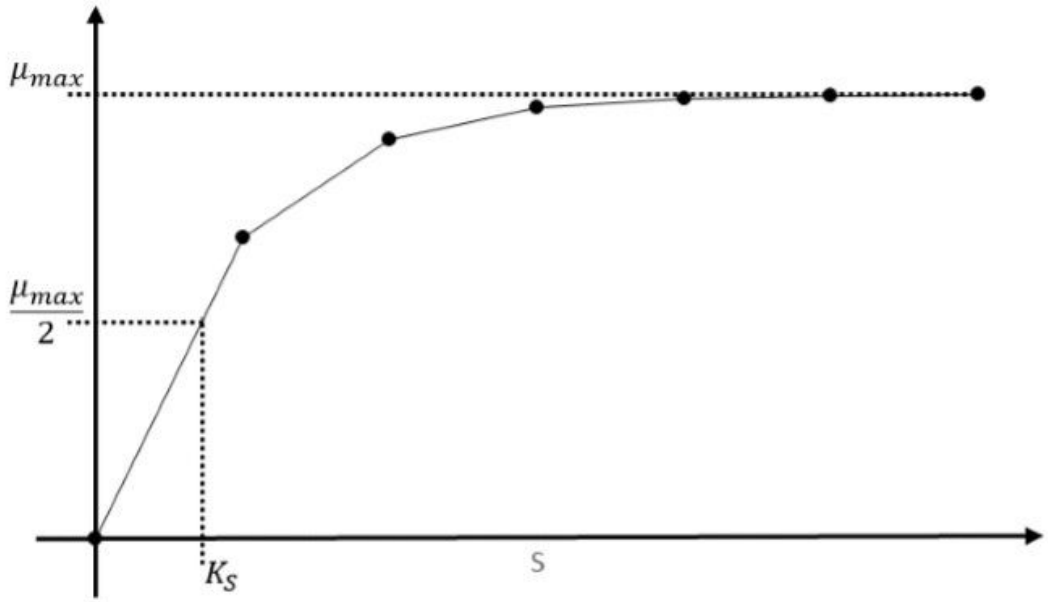

Figure 1

General curve for cell growth variation as a function of the substrate concentration from Braga12.

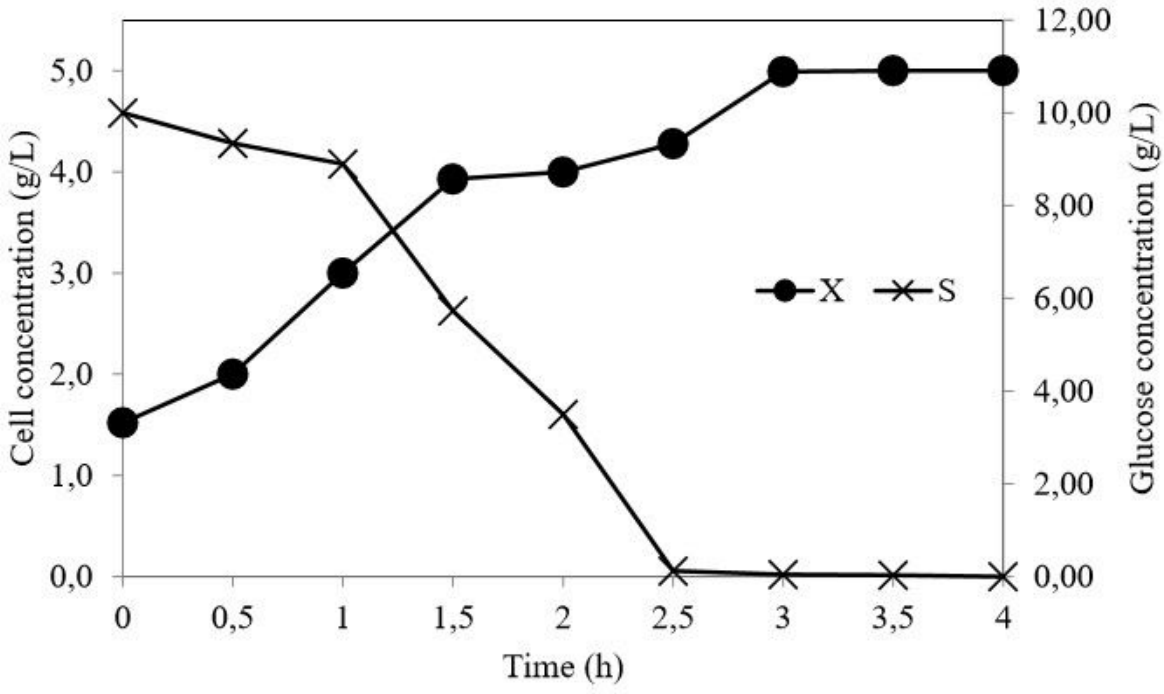

Figure 2

Experimental data obtained from a Saccharomyces cerevisiae culture on an airlift bioreactor with an initial substrate concentration of 10 g.L-1, a gas and reactor volume proportion of 3 vvm, and an air flux of 15 L.min-1 8.

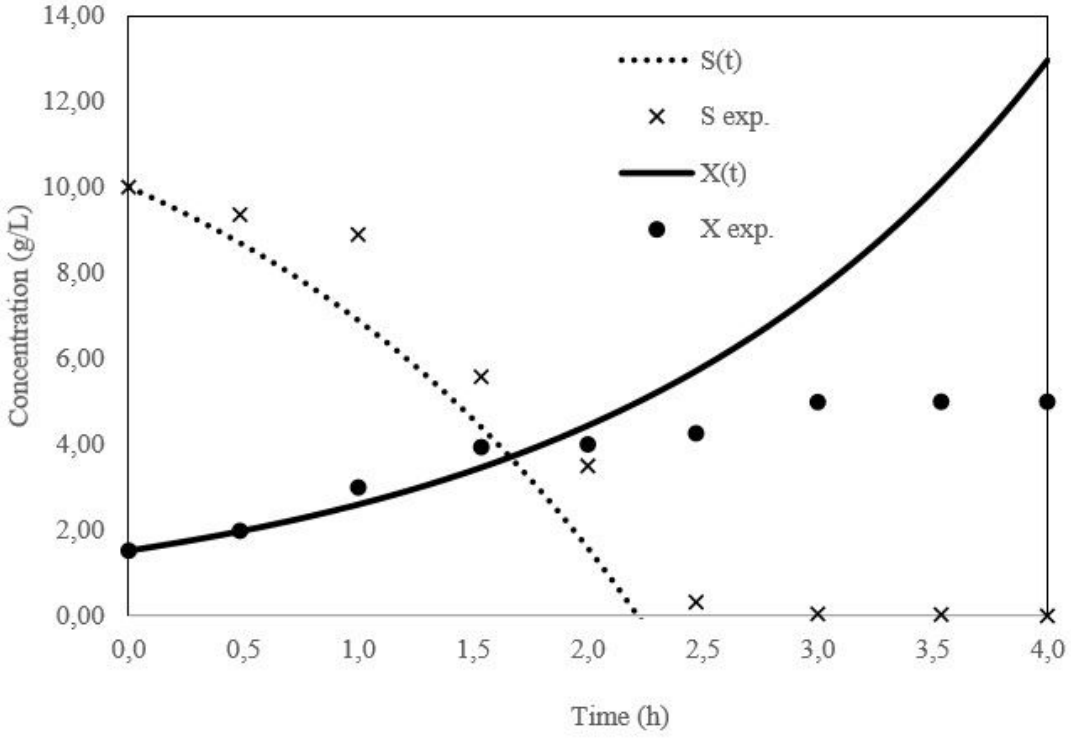

Figure 3

Comparison of the continuous Monod model and the experimental points (Experiment 4).

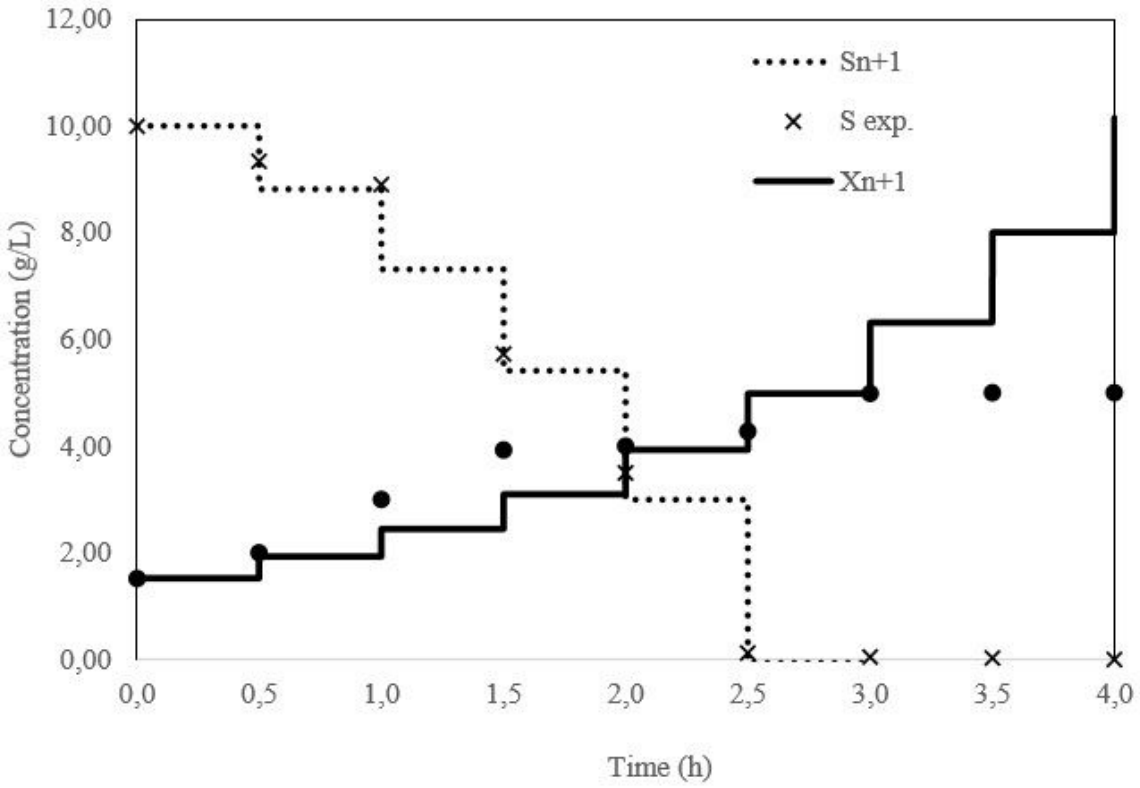

Figure 4

Comparison of the discrete Monod model and the experimental points (Experiment 4).

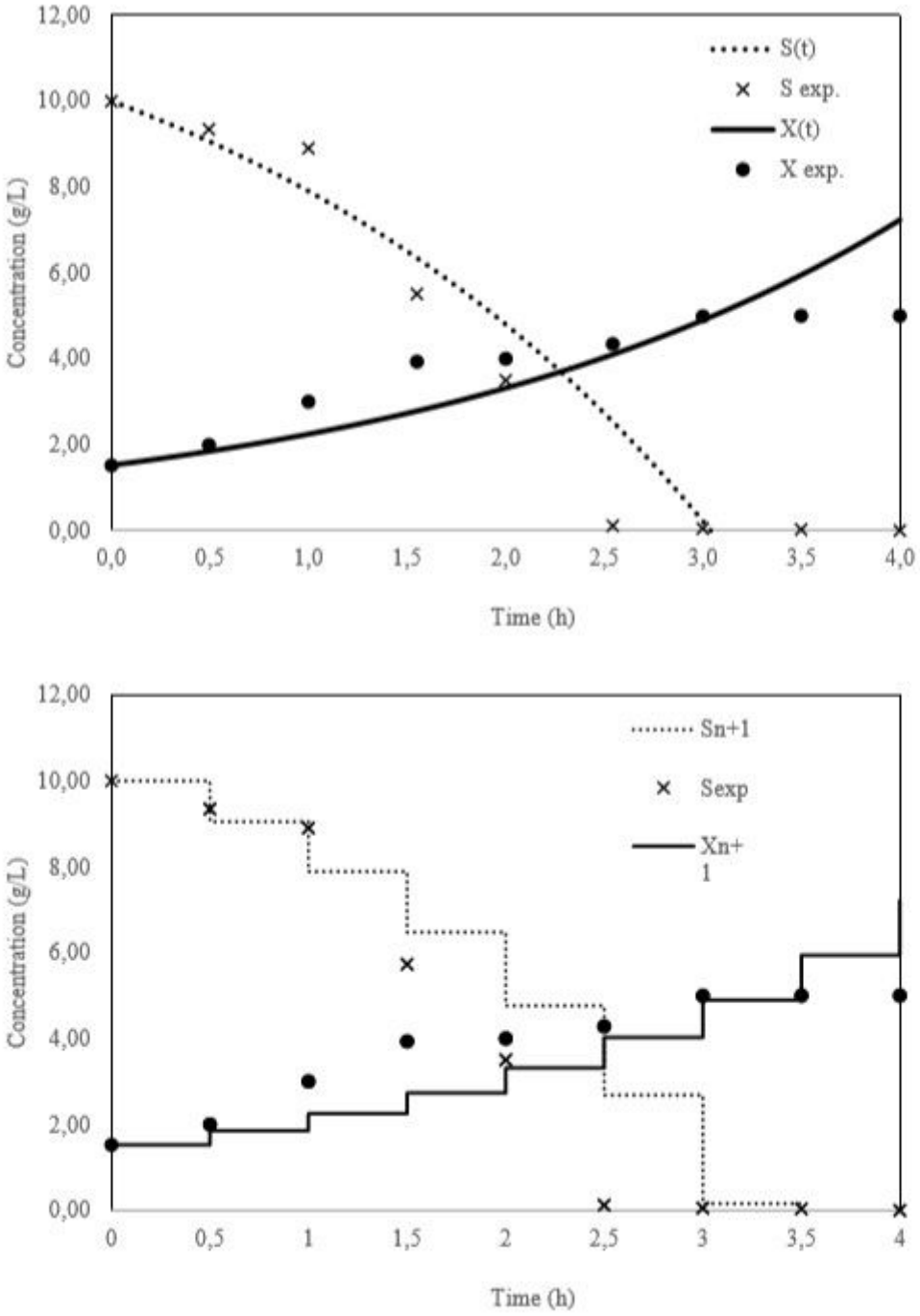

Figure 5

Comparison of the Andrews models (discrete and continuous) and the experimental points (Experiment 4).

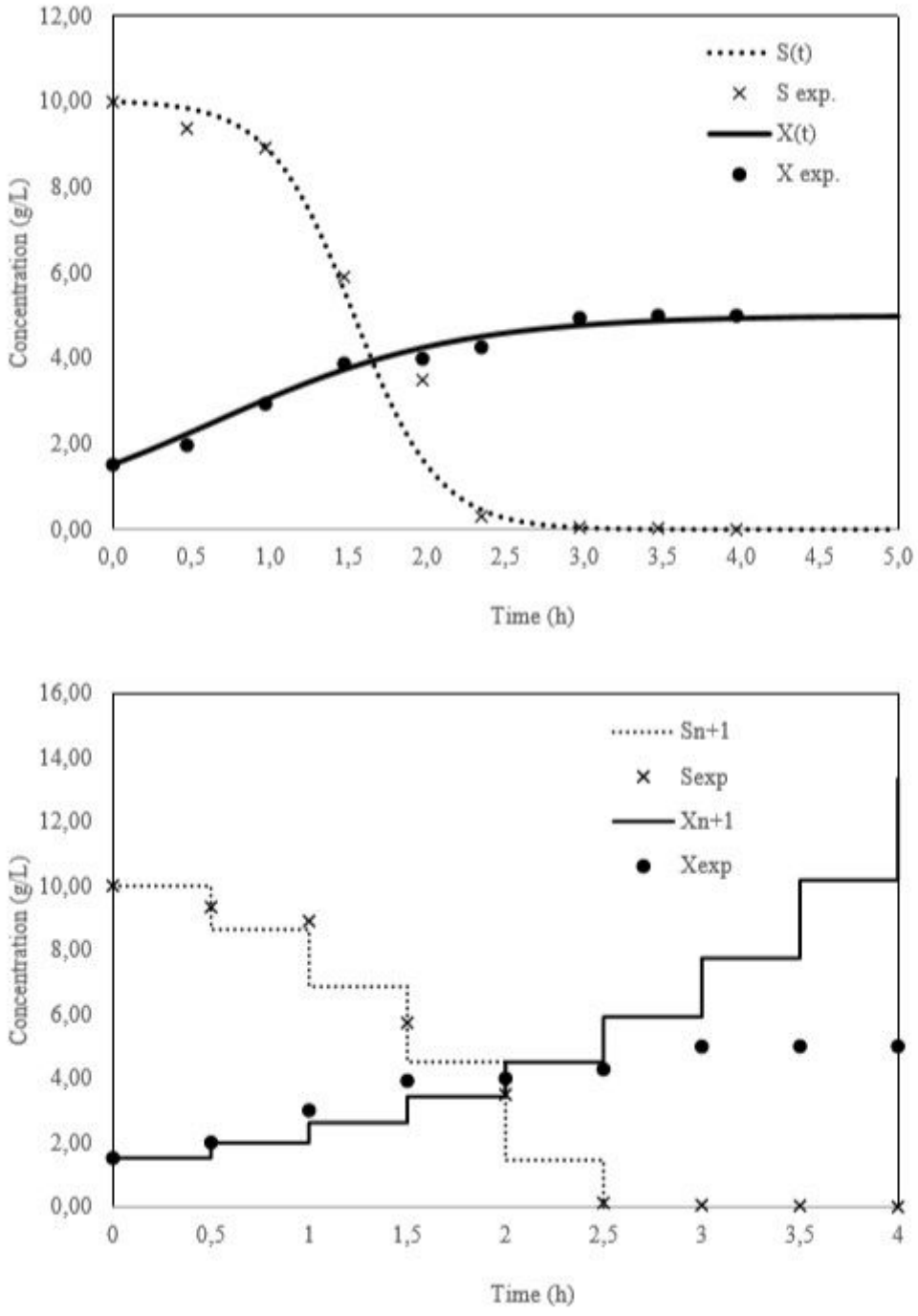

Figure 6

Comparison of the Verhulst models (discrete and continuous) and the experimental points (Experiment 4).

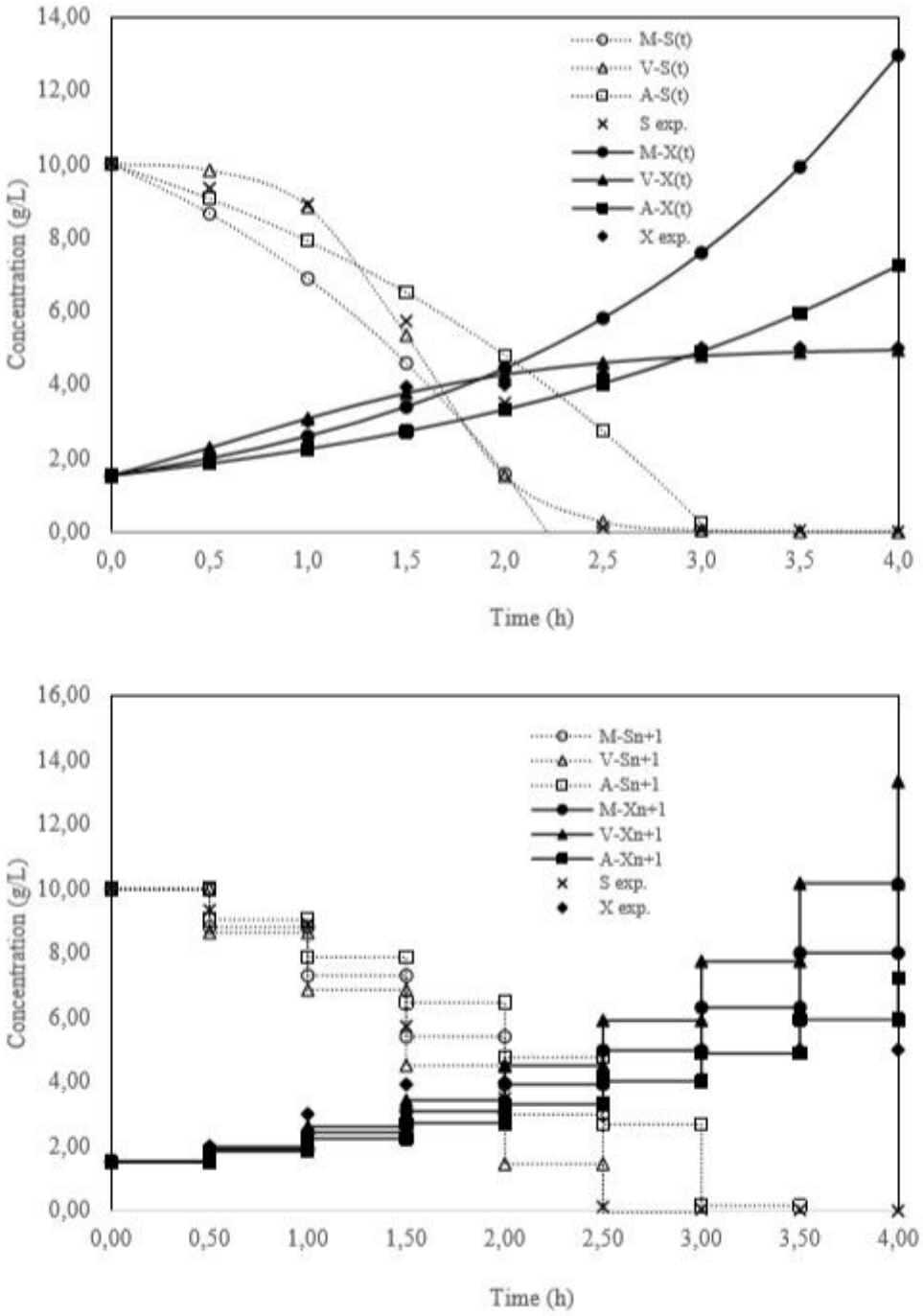

Figure 7

Comparison of all the continuous and discrete models.

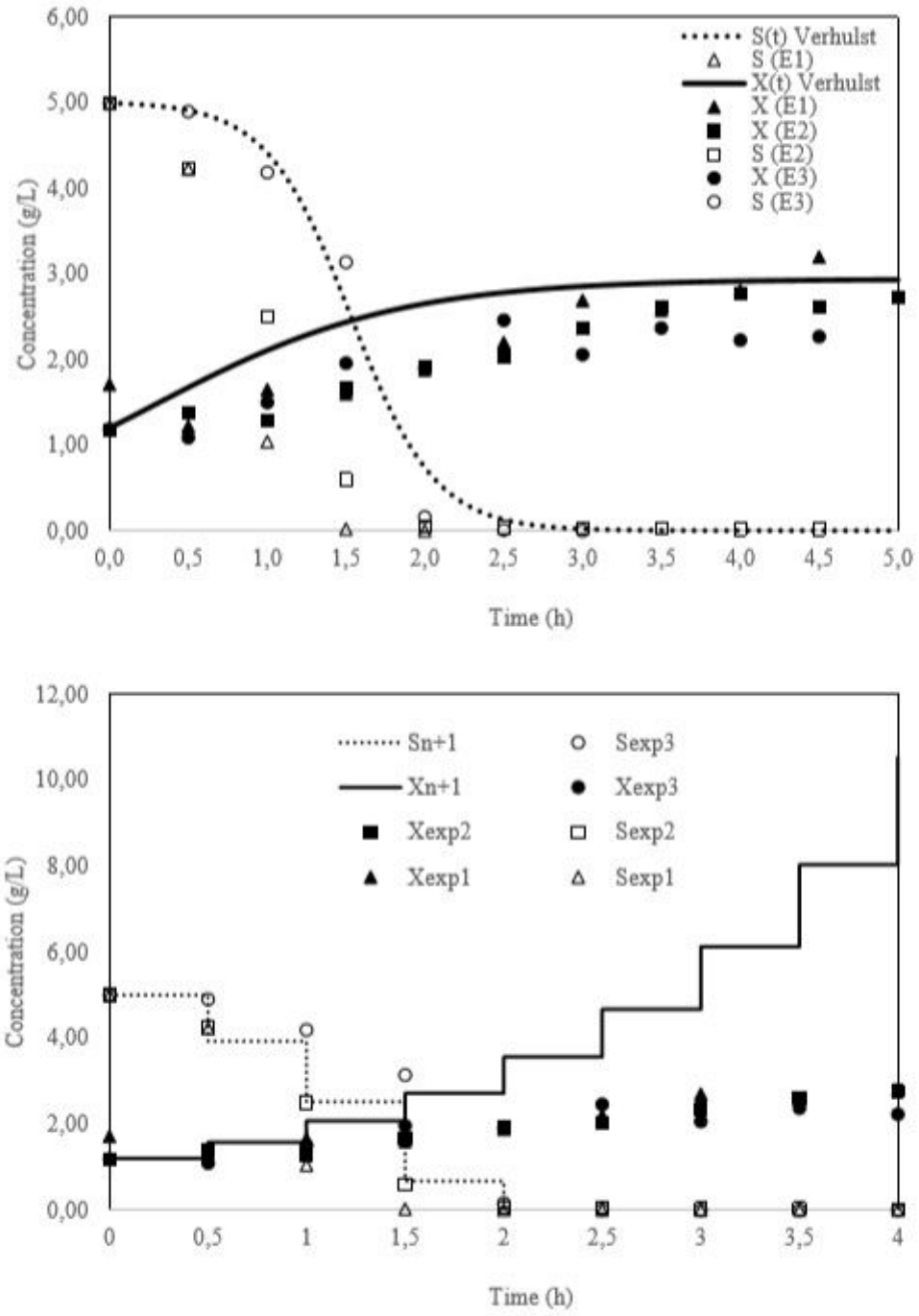

Figure 8

Simulation of the continuous and discrete Verhulst models for an initial cell concentration of 1.2 g.L-1 and an initial substrate concentration of 5 g.L-1 and comparison with experiments 1, 2 and 3.

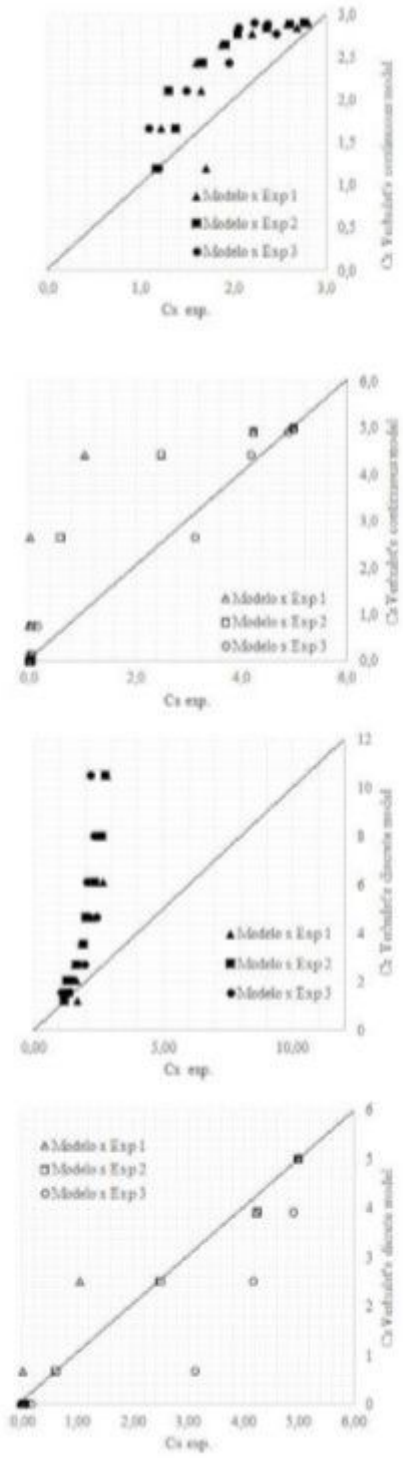

Figure 9

Dispersion chart for the accuracy of the Verhulst model. The initial cell concentration is 1.2 g.L-1, and the initial substrate concentration is 5 g.L-1.